Cluster dynamics on vicinal surfaces

Steven Kenny
The Blackett Laboratory, Imperial College, London SW7 2BZ, United Kingdom

Mark R. Wilby
Department of Electrical and Electronic Engineering, University College, Torrington Place, London WC1E 7JE, United Kingdom

Andrea K. Myers-Beaghton and Dimitri D. Vvedensky
The Blackett Laboratory, Imperial College, London SW7 2BZ, United Kingdom

(Received 21 February 1992)

We have carried out a study of the dynamics of cluster formation during epitaxial growth and recovery on vicinal surfaces. By considering all of the possible configurations for up to four-atom clusters, we have been able to elucidate the role of different island types and shapes during the various stages of growth. Inclusion of species with slow decay pathways is crucial for describing the recovery of the surface morphology, since the breakup of stable configurations is the rate-determining step for the relaxation of the surface once the incoming flux has been turned off. We find that the recovery of the surface can be divided into two stages: an initial rapid decay due to activity of atoms with one nearest neighbor, and a subsequent slower stage is coupled up to third order to the breakup of the most stable species.

I. INTRODUCTION

Molecular-beam epitaxy (MBE) on vicinal surfaces provides a rich arena for exploring the mechanisms of epitaxial growth. Atoms that are deposited on the crystal surface acquire a certain amount of kinetic energy from the thermal vibrations of the substrate. This energy affords the atoms a degree of mobility through the process of diffusion. If the average time between the interarrival of atoms on the terraces is sufficiently large, then the atoms have a higher probability of reaching the step edge than of forming a nucleation center with other migrating atoms. In this case, growth proceeds in a mode that is called step advancement. Alternatively, if the interarrival time of atoms from the incident beam is sufficiently small, then the encounter probability of atoms on the terraces is large, leading to atomic collisions that form nucleation centers that act as traps for other migrating atoms. Growth thereby proceeds by the formation, accretion, and coalescence of clusters. This physical picture identifies[1,2] the diffusion constant and the flux as the important physical quantities for developing a systematic analytic formulation of epitaxial growth on vicinal surfaces.

The theory of Burton, Cabrera, and Frank (BCF),[3] and corrections thereto,[4–10] are the usual starting points for a theoretical model for MBE on vicinal surfaces. The BCF theory describes the near-equilibrium growth of crystals on stepped surfaces. Since stepped surfaces, with a misorientation of a few degrees, are frequently used as substrates in MBE, there has been a renewed interest in applying the BCF-type theories to MBE. The BCF theory[3] is based on a diffusion equation for the adatom concentration and is formulated subject to three assumptions: (i) the effect of the moving boundary can be neglected, (ii) the concentration at the step edge is at equilibrium, and (iii) there are no interactions or reactions among the adatoms. These simplifying assumptions allowed an analytical solution to be obtained for the step velocity and for the growth rate to be calculated.

It has been recognized that the formation of clusters under MBE conditions plays an important role in the evolution of the surface.[2,5,9,10] Cluster formation was originally modeled within the BCF framework by taking into account only diatomic island formation[2] and, more recently, by considering formation of islands with large numbers of atoms.[9,10] These models have found success in predicting the point of transition to the step propagation mode,[2] since the transition to growth by step advancement is taken as being the point at which cluster formation can be ignored.

Fuenzalida[10] calculated cluster distribution functions in the steady-state limit without imposing an upper bound on the size of the cluster considered. In this model, only attachment processes were considered; detachment from neither clusters nor step edges was included, so only growth under relatively high deposition rates with no recovery could be treated. Nevertheless, this work does generalize that of Ref. 2, where only diatomic clusters are considered within this framework. This works is also consistent with and complementary to that in Ref. 9, in the qualitative profile of the cluster distribution function both in the region of step flow as well as in a regime with significant cluster growth.

In previous studies,[2,9,10] only one representative type of each cluster of a particular size was considered. However, for islands composed of three or more atoms, there are several possible island shapes. Differently shaped islands, even if composed of the same number of atoms, would be expected to have different formation and breakup rates because the active sites involved have different barriers. This would not be expected to have a great

effect during growth, as simulation studies indeed verify Ref. 11. However, during the recovery period after cessation of growth, the pathway toward equilibrium,[11,12] and the equilibrium state, itself, would be expected to be strongly dependent upon including the shape-dependent kinetic rates of the islands.

In this paper, the theory developed in Refs. 2 and 9 is extended to take into account the different possible island configurations in order to study the relative importance of the various island shapes during growth. The formation of islands of up to four atoms is considered in detail, since under the growth conditions we model here (i.e., near the step propagation mode), the formation of larger clusters may be neglected.[9,10] The effects of step and island breakup have also been included in this model, thus rendering it valid for the study of the relaxation of the surface upon cessation of the incident beam. We show that consideration of the different island configurations is particularly important in forming a realistic picture of recovery of the surface. The relaxation of the surface is found to be dominated by the decay of the most stable cluster to which the decay of other island types is coupled.

The outline of the paper is as follows. In Sec. II, we will show how the original model used in Refs. 2 and 9 can be extended to consider detailed island formation and decay for up to four-atom islands. The approach adopted here is similar to that used in Refs. 2 and 9 in that a reaction-rate formalism is used to identify the various steps in the growth process as reactions among the pertinent species. This allows us to distinguish different types of clusters by their lifetimes and their decay pathways. The main body of results is contained in Sec. III. The results obtained from the numerical integration of the model equations are discussed for growth and recovery in terms of the density of different types of islands under growth conditions where growth is dominated by step advancement. Our conclusions are summarized in Sec. IV.

II. THE MODEL

As in earlier work,[2,9] the growth model is built by identifying the kinetic processes taking place on the vicinal surface, which are then described in terms of "reactions" among the various "species." The species include the atoms from the molecular beam and the individual island types, including single adatoms on the surface. Each process in the growth is then described by a reaction that involves the conversion of these species among one another, with appropriate constants.

The processes occurring on the surface can be categorized as follows: deposition of atoms from the beam, diffusion of the adatoms on the surface, formation and breakup of islands, and the attachment and detachment of adatoms from the step edges. The evaporation of atoms is neglected as, under typical growth conditions of MBE, this process can be neglected. For example, the lifetime of Si atoms on a Si surface has been estimated as 10^7s.[13] We will use a notation where an island made up of j atoms will be denoted by Y_j and atoms from the incoming beam will be denoted by A. In particular, a free atom on the surface is signified by Y_1. The growth kinetics can therefore be described by the following reaction sequence:

$$A \xrightarrow{k_0} 2Y_1, \quad A + Y_j \xrightarrow{k_j} Y_{j+1}, \quad Y_1 + Y_j \underset{q_j}{\overset{r_j}{\rightleftarrows}} Y_{j+1} \qquad (1)$$

for $j = 1,2,\ldots,N$, where atoms including only up to N atoms are considered. The consistency of this restriction will be discussed below. Reactions involving the species A represent the deposition process. The first reaction describes the adsorption of single atoms from the beam onto the substrate, with the creation of a free surface adatom Y_1. The rate of this reaction, k_0, and those of the other reactions in (1), will be discussed below. The second reaction accounts for the deposition of arriving atoms onto a site adjacent to either a substrate atom or island, which leads to the formation of a diatomic island or a larger island, respectively. The absence of desorption in our model means that the back reactions in these first two reactions have been omitted. The forward direction of the third reaction accounts for the collision of a migrating adatom with either another adatom or an island to form an island with one additional atom. The back reaction describes the detachment of an atom from an island with the creation of a single adatom and an island with one less atom. Attachment and detachment processes involving more than a single atom have not been included.

The reactions in (1) are quite general, but exclude two important effects: the kinetic processes at the step edge and the migration of the single adatoms. The first process is included in the boundary conditions, which will be specified below, while the second is included in constructing the master equation for the joint probability distribution function for the Y_j,[14] as in Ref. 9. In constructing the master equation, a coarse graining is performed wherein the vicinal surface is divided into cells along the direction of the steps. Thus, we will describe the diffusion process as a cell-to-cell hopping, with the cells having an infinite extent along the steps, so that we have no spatial resolution along this direction. In effect, we are performing an average of the concentrations of the Y_j along the step direction, so the central quantities are the average concentrations of the species Y_j in the ith cell at time t, which is signified by $n_j^i(t)$. The equations of motion for the $n_j^i(t)$ are obtained from the master equation as

$$\begin{aligned} \frac{dn_1^i}{dt} &= \sum_j D_{ij} n_1^i + R_1^i(n_1^i, n_2^i), \\ \frac{dn_j^i}{dt} &= R_j^i(n_1^i, n_2^i, \ldots, n_N^i), \end{aligned} \qquad (2)$$

where $j \geq 2$. The reaction contributions R_j^i, all of which are local to the ith cell, are given by

$$
\begin{aligned}
R_1^i(n_1^i,n_2^i)&=-2r_1(n_1^i)^2-k_1n_1^i+k_0A+2q_2n_2^i\ ,\\
R_j^i(n_1^i,n_{j-1}^i,n_j^i,n_{j+1}^i)&=n_1^i(r_{j-1}n_{j-1}^i-r_jn_j^i)\\
&\quad+k_{j-1}An_{j-1}^i-k_jn_j^i\\
&\quad+q_{j+1}n_{j+1}^i-q_jn_j^i\ ,\\
&\qquad j=2,\ldots,N-1\ ,\\
R_N^i(n_1^i,n_{N-1}^i,n_N^i)&=r_Nn_1^in_{N-1}^i+k_{N-1}n_{N-1}^i-q_Nn_N^i\ ,
\end{aligned}
\tag{3}
$$

where we have used the symbol A to signify the concentration of A atoms. By taking the continuum limit of these equations, we obtain a set of coupled nonlinear diffusion equations for the quantities $n_j(x,t)$, where x is the running coordinate along the terrace $0\le x\le h$:

$$
\begin{aligned}
\frac{\partial n_1}{\partial t}&=D\frac{\partial^2n_1}{\partial x^2}+J+\tilde{R}_1(n_1,n_2)\ ,\\
\frac{\partial n_j}{\partial t}&=R_j(n_1,n_{j-1},n_j,n_{J+1})\ .
\end{aligned}
\tag{4}
$$

In writing the first of these equations, we have separated out the contribution of the flux, which is denoted by J, and the reaction contribution without this flux term is now denoted by $\tilde{R}_1$. The term including the adatom diffusivity D accounts for the migration of the adatoms on the surface. We take D to have the Arrhenius form

$$D=\nu a^2\exp(-E_D/k_BT)\ , \tag{5}$$

where ν is an adatom vibrational frequency on the order of 10^{13} s^{-1}, a is the nearest-neighbor hopping distance, E_D is the effective activation energy for diffusion of a long adatom, k_B is Boltzmann's constant, and T is the substrate temperature. The rate constants k_j and r_j were derived in Refs. 2 and 9, with the result that

$$k_j=Ja^2m_j\ , \tag{6}$$

where m_j is the number of sites around the species Y_j that will form a species Y_{j+1} when filled. This quantity clearly depends on the shape of the island, as will be discussed further below. For the r_j, we obtained

$$r_j=\sigma_jD\ , \tag{7}$$

where σ_j is the capture efficiency of a j-atom island, which we take to be a constant of order unity.

Finally, it is convenient to move into a frame that moves with the steps. Because we omit evaporation and because we allow growth to occur only on a single layer on any one terrace, after the deposition of a monolayer of material, the steps have advanced one terrace length (on average). Thus, by changing to a coordinate system that moves with the velocity of the steps, we can monitor the evolution of individual terraces rather than have terraces move by. This has the additional beneficial effect of making the concentrations of the various species constant in the steady state. The velocity includes contributions from both the flux of mobile atoms to the step edge as well as the effect of incorporating immobile islands. The time-dependent velocity $v(t)$ is given by[7]

$$v(t)a^2=\left[D\frac{\partial n_1(x,t)}{\partial x}+v(t)\sum_{j=1}^{N}jn_j(x,t)\right]\Bigg|_{x=h}^{x=0}\ , \tag{8}$$

where h is the terrace length. The first term on the right-hand side of (8) is the flux of mobile adatoms into the step from above and below. There is no such term for the island as they are assumed to be immobile. The second term is the convective flux of material into the step, i.e., the adatoms and the islands swept up by the moving step. Thus, changing to the moving frame, $x\rightarrow x-vt$, Eq. (4) become

$$
\begin{aligned}
\frac{\partial n_1}{\partial t}&=D\frac{\partial^2n_1}{\partial x^2}+J+v(t)\frac{\partial n_1}{\partial t}+\tilde{R}_1(n_1,n_2)\ ,\\
\frac{\partial n_j}{\partial t}&=v(t)\frac{\partial n_j}{\partial t}+R_j(n_1,n_{j-1},n_j,n_{j+1})\ .
\end{aligned}
\tag{9}
$$

There are several features of the set of equations in (9) that are worth noting. First, these equations take the form of rate equations[15] with diffusion. The spatial dependence in the solution of these equations caused by the presence of the diffusion term is necessary because of the spatial inhomogeneity induced by the finite terraces. If the terrace length was extended to infinity, then this inhomogeneity would disappear and the equations would reduce to conventional rate equations. Second, Eq. (9) are mean field in character in that there are no stochastic terms from either the deposition flux or the diffusion, although both sources of stochasticity are included in the master equation.[14] Comparisons between quantities calculated without these noise terms and averages over full simulations[16] show good qualitative agreement, so we do not anticipate any gross inaccuracies by omitting these terms in our study.

To solve (9) we require boundary conditions at the step edges above and below the terrace edges. These are determined by writing attachment and detachment reactions for the adatoms above and below the step edges. Details of the expressions used for the rates of attachment and detachment are as given in Ref. 9; as before, we assume that the reactions at attachment and detachment from the step edge are symmetric and that, on average, the step morphology remains the same throughout the growth; otherwise an explicit two-dimensional treatment would be required.

We now consider in more detail the expressions for the island formation and breakup rates q_j. Previously,[9] only one representative type of cluster of a particular size was considered, with growth and decay rates being the same for all species. For a detailed treatment of the cluster dynamics on the surface, one must recognize that for islands with greater than two atoms, there are several possible island configurations. These are shown in Fig. 1 for up to four-atom islands. We will denote the shape of islands (straight, square, L shaped, Z shaped, etc.) with $j\ge3$ with an additional letter subscript as shown in Fig. 1.

For island formation, whether through deposition of an arriving atom onto a neighboring site or through collision of a migrating adatom, we must now consider the fact that different island shapes will have different proba-

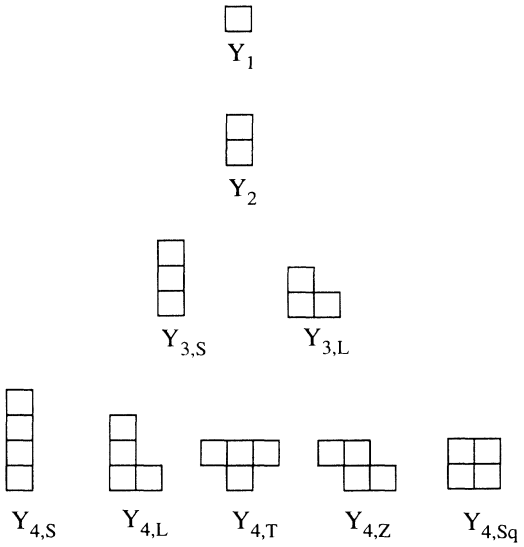

FIG. 1. Possible configurations for islands with up to four atoms.

bilities of being formed. As in (6), k_j (for $j \geq 1$) is related to the number of sites around an island of j atoms that will form a $(j+1)$-atom island when filled by a depositing atom, a quantity we have denoted as m_j. Here, we calculate m_j by counting the nearest neighbors of the cluster; thus, $m_1=4$, $m_2=6$, etc. Thus, the total rate of the reaction $Y_j + A \rightarrow Y_{j+1}$ by deposition at an incoming flux J is given by $Ja^2 m_j n_j$, as explained in (6). However, we must weigh the formation of the different configurations of Y_{j+1} by their probabilities of forming, which are given in Fig. 2. Similarly, for island formation due to a collision with a migration adatom, the total reaction rate for $Y_j + Y_1 \rightarrow Y_{j+1}$ which, as before,[2,9] we take to be proportional to the diffusivity $Dn_1 n_j$, must also be weighted by the number of positions around the cluster which will result in a particular Y_{j+1} island shape when collision and sticking occurs there.

Figure 3 shows the island breakup reactions for the various island shapes for up to four-atom clusters. In addition to allowing for the detachment of one atom to form a free adatom and the next-largest island, the possibility of island breakup liberating more than one adatom must also be taken into account. For islands with four atoms, deformation to form an island of the same size but of a different configuration must also be included. The breakup and deformation-rate constants are estimated by combining the possibilities of each constituent atom breaking away and hopping to an adjacent unfilled site. We assume that nearest-neighbor hopping only is allowed. Nucleation upon existing clusters is considered too unlikely at the growth conditions considered here. This assumption is implemented explicitly by preventing constituent atoms diffusing onto other atoms contained within clusters, rather than the step itself. An Arrhenius expression is used to estimate the energy barrier to detachment from the cluster. If the energy between two nearest-neighbor atoms is E, then this yields

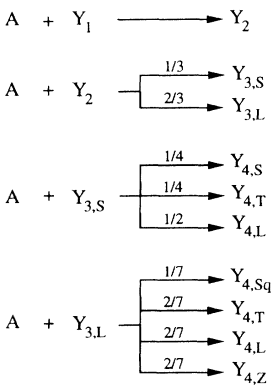

FIG. 2. Reactions for formation of islands by adatom deposition showing the probabilities of forming different islands shapes.

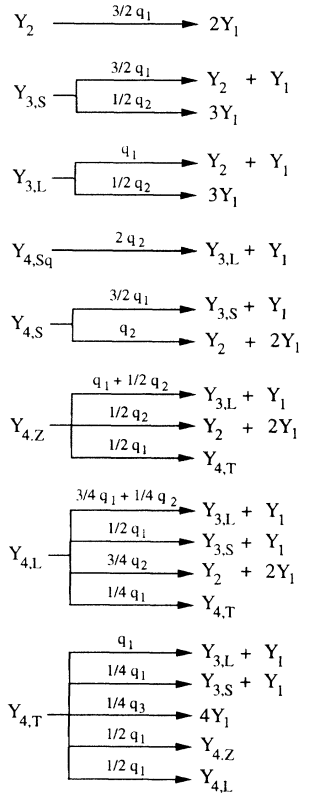

FIG. 3. Reactions and rate constants for island breakup and rearrangement, where ν_n is given in (9).

$$\nu_n = \nu \exp[-(E_D + nE_N)/k_B T] \tag{10}$$

for the frequency of an adatom with n bonds to the cluster to detach itself and hop in one of the four neighbor directions. To obtain the total decay rate of one species to another, we must consider which hops of which constituent atoms of the cluster will result in formation of the product. For example, consider the case of a linear cluster of three atoms, i.e., $Y_{3,S}$, decomposing to an adatom and a diatomic island. This can occur by the movement of either of the two end atoms to any one of three of its four neighboring sites. In both cases this involves the

breaking of a single bond. Combining, we obtain

$$q(Y_{3,S} \rightarrow Y_2 + Y_1) = 2 \times \tfrac{3}{4} \times \nu \exp[-(E_D + E_N)/k_B T] = \tfrac{3}{2}\nu_1 \ . \quad (11)$$

Alternatively, the central atom in $Y_{3,S}$ causes decay of the island into three free adatoms by hops in two out of four directions; thus,

$$q(Y_{3,S} \rightarrow 3Y_1) = \tfrac{1}{2}\nu_2 \ . \quad (12)$$

This reaction is much slower, since the adatom must overcome a larger energy barrier of $E_D + 2E_N$ to break away.

It is important to recognize that of all the islands considered, at least one decay pathway is proportional to ν_1 with the important exception of the square four-atom island $Y_{4,\mathrm{Sq}}$, for which the decay pathways are all proportional to ν_2. This is a consequence of its compact shape, giving all constituent atoms two nearest neighbors. However, even for clusters containing more atoms, if a singly bonded atom is not present, then there must be at least four doubly bonded atoms as well as the triply bonded and fully coordinated atoms. This means that regardless of its size, any cluster must have a decay pathway proportional to at least ν_2, and possibly ν_1. The decay of one cluster into another is governed by these two rates, so the simplified system we consider, which is applicable only to the growth regime near step flow, also contains all the relevant physical behavior of the more complex clusters.

The recovery stage of growth takes place when the beam is switched off. The study of the recovery of the surface involves omitting the terms due to the deposition of atoms, these being the formation of adatoms by the deposition of atoms onto the substrate and those terms that represent the deposition of atoms onto sites adjacent to adatoms or islands. This is done by removing the flux term and setting m_J to zero for all islands in (1).

III. RESULTS AND DISCUSSION

In order to discuss the results obtained from the modeling of MBE growth, it is first necessary to define the various stages of growth on a stepped surface, illustrated in Fig. 4. The first stage, the transient period of growth, occurs immediately after the beam is switched on. This stage encompasses the initial buildup of material on the surface (the period where the coverage rises rapidly) and any subsequent period where the coverage may oscillate before settling to its steady-state value. The second stage of the growth is the steady-state period where the coverage and the step-edge velocity are both at constant nonequilibrium values. The third stage of the growth is the relaxation of the surface, in which the coverages of the various species decay towards their equilibrium values, the final stage being the equilibrium period where the coverage remains constant.

The results of this model of MBE have shown some surprising aspects about the role of different islands and island shapes in the evolution of the stepped surface. It becomes evident when studying the role of the islands in the growth that different configurations will be of varying

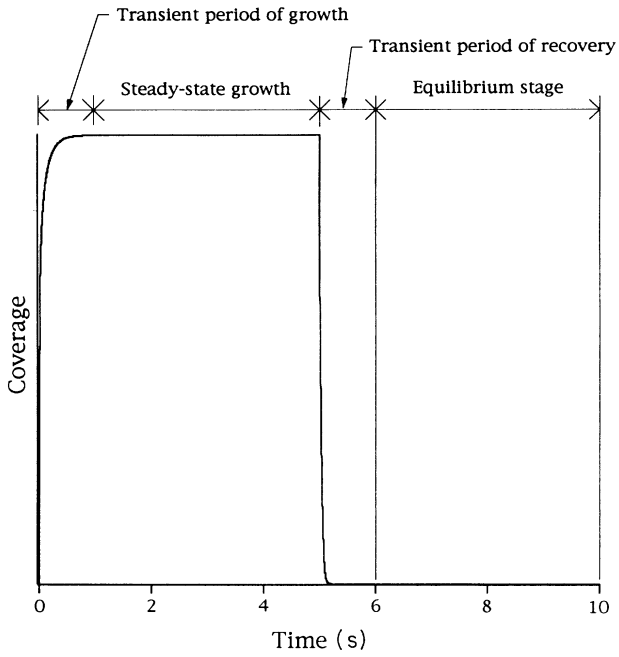

FIG. 4. Schematic of the various stages of surface growth and recovery.

significance, and also that their importance will depend not only on the growth conditions, but on the stage of the growth. We now proceed to discuss the role of the different island shapes in the early stages of the growth, during steady-state growth, and during the relaxation of the surface to equilibrium. Since the concentration of each species $n_j(x,t)$ depends on the position on the terrace, we will consider the total coverage of the terrace with a particular species as

$$\theta_j(t) = \frac{a}{h} \int_0^h n_j n_j(x,t) dx \ , \quad (13)$$

where h is again the terrace length.

During the early stages of growth, just after the beam is switched on, the emphasis is on the formation rates of the different island species. Figure 5 shows the coverages of various islands in the early period of growth at 700 K, and it is apparent that the more readily formed island configurations are responsible for most of the coverage in the early stages of growth. As illustrated in Fig. 2, the $Y_{3,L}$ islands are twice as likely as straight $Y_{3,S}$ islands to be formed from collisions of depositing of migrating atoms with Y_2 islands, and they therefore dominate the surface morphology. Similarly, for the four-atom islands, in the early stages of growth the less easily formed configurations such as the square $Y_{4,\mathrm{Sq}}$ are sparser on the surface than the more readily formed $Y_{4,L}$. Also, the larger islands have considerably longer transient times.

At steady state, the island breakup reactions (shown in Fig. 3) become important and island decay must balance its formation rate. Cluster stability now plays an important role, and the more stable island configurations will dominate. The steady-state concentrations of the three-atom and four-atom clusters, including the relative amounts of the different island shapes at 700 and 750 K,

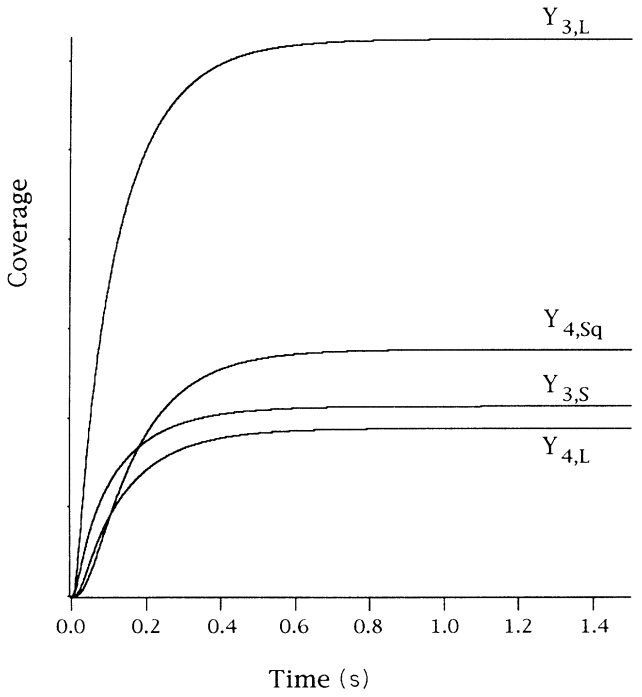

FIG. 5. Early stages of surface growth at $T=700$ K, $J=1$ monolayer/s, $E_D+1.3$ eV, $E_N=0.26$ eV, with a terrace width of $h=18a$.

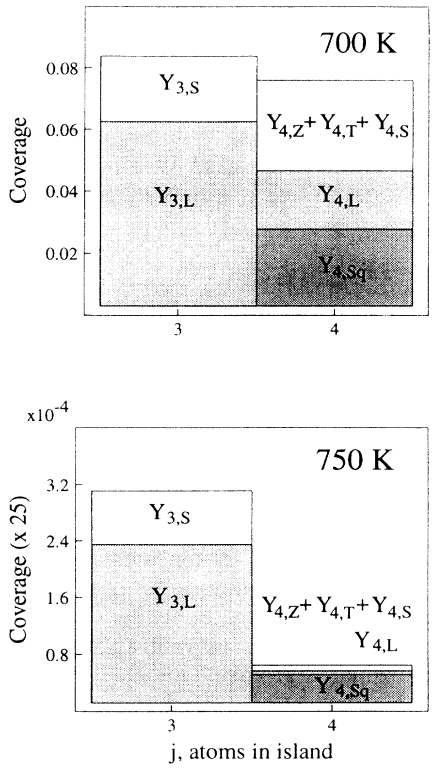

FIG. 6. Steady-state coverages for three- and four-atom clusters at $T=700$ and 750 K with the same parameters and growth conditions as for Fig. 5. Note the difference in scale; the results at 750 K are magnified 25 times with respect to those at 700 K.

are shown in Fig. 6. It is immediately apparent that as the temperature increases, the concentration of the larger clusters relative to that of the smaller ones decreases. The fact that there is a temperature range where the calculated concentrations decay with increasing size justifies our original approach of using only a limited number of clusters. However, there will be a temperature below which the steady-state concentrations will increase rather than decrease with cluster size, thus indicating that the growth mode is far from step flow. In such circumstances the reactions of larger clusters cannot be ignored and our simplifying assumptions will be inaccurate. Considering different clusters of the same size we notice that the more stable clusters dominate as the temperature is increased. In the case of the four-atom clusters the relative fraction of $Y_{4,\mathrm{Sq}}$ to that of the total concentration dominates at 750 K, whereas at 700 K it is comparable to all the other four-atom cluster concentrations.

The study of the role of islands in the relaxation of the surface yielded the most interesting results. The process of surface relaxation turns out to be a coupled reaction between the various island configurations. Figure 7 shows the logarithm of the various cluster coverages as a function of time, as the surface relaxes at a temperature of 750 K. It is obvious that the concentration rapidly becomes much too small to have any physical significance on the system. However, the overall behavior shows some interesting features that should be a general effect of the recovery process. In addition to this, the initial stages of the recovery shown in the inset of Fig. 7 explains the double exponential form frequently used to analyze the recovery profile as measured by reflection high-energy electron diffraction.[17–20]

It is apparent that the recovery can be divided into several distinct stages. After the beam is switched off, there is an initial transient period of relaxation, shown more clearly in the inset. In this stage, the clusters decay rapidly since the supply of adatoms from the beam leading to island formation has been cut off and excess adatoms on the surface are incorporated into the step edges. The initial decay of the coverage is steep and falls as $\exp(-f\nu_1 t)$, where f is a fraction depending on the shape of the cluster, as shown in Fig. 3, and ν_1 is the decay rate for detachment of atoms with one nearest-neighbor bond, as given in (10). The exception is the $Y_{4,\mathrm{Sq}}$ which, as can be seen in Fig. 3, does not possess a fast-decay pathway with a rate proportional to ν_1, and instead decays at a rate proportional to ν_2.

At the end of the first stage of recovery, due to their fast-decay pathway, the concentration of all cluster types falls below that of $y_{4,\mathrm{Sq}}$, which decays at the much slower rate of $\exp(-2\nu_2 t)$. Once the concentrations of the adatoms and clusters have dropped below $n_{4,\mathrm{Sq}}$, the decay of the square four-atom clusters creates a supply of smaller islands and adatoms, which may then recombine to form larger clusters. Consequently, in the second stage of recovery the decay rates of all the surface concentrations of the various island types now become linked to the decay of the clusters.

The coupling reactions linking the various decays are

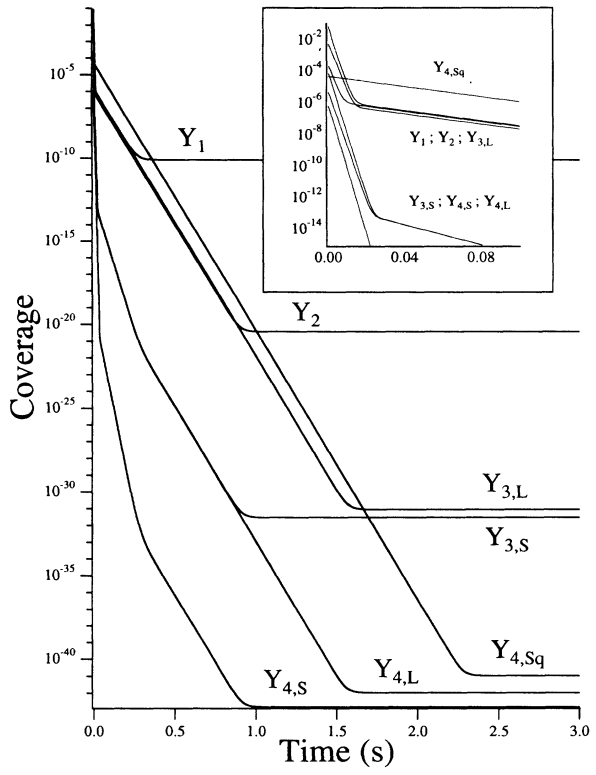

FIG. 7. Decay of the surface coverage of various island types during relaxation of the surface at $T=750$ K with the same parameters and growth conditions as for Fig. 5. The inset graph shows the first tenth of a second.

shown in Fig. 8. The vertical pathway shows the products formed by the slow decay of the square four-atom clusters, and the horizontal pathways show some of the recombination reactions. Since all of the reactions shown in Fig. 8 will be fast compared to the initial breakup reaction at a rate of $2\nu_2$, this is the rate-limiting step and the decay of the other species will be coupled to this decay reaction. The adatom and diatomic cluster concentrations formed during this stage by the decomposition of

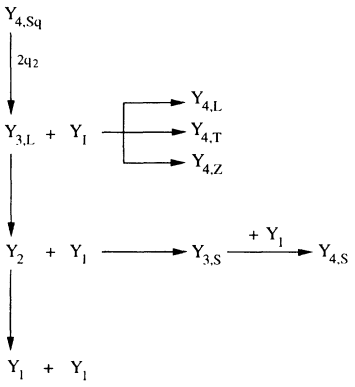

FIG. 8. The coupled formation and decay reactions that determine the surface evolution during relaxation.

the four-atom squares at a rate drops as $\exp(-2\nu_2 t)$. As such, this is the rate-determining step in the evolution of the different species and therefore corresponds to their decay rate. Figure 7 and 8 show that the clusters that have a decay of $\exp(-4\nu_2 t)$, such as $Y_{3,S}$, are formed by two of the species found in the decay of the square four-atom islands. Since the formation of rate of these larger island is proportional to the concentrations of the reactant, second-order coupling occurs and these species decay at the faster rate of

$$[\exp-(-2\nu_2 t)]^2=\exp(-4\nu_2 t)\ . \tag{14}$$

Third-order coupling, i.e., a decay rate proportional to

$$[\exp(-2\nu_2 t)]^3=\exp(-6\nu_2 t)\ , \tag{15}$$

occurs for the $Y_{4,S}$ species in the second recovery stage, as can be understood by following its reaction path in Fig. 8. Thus, the breakup of the $Y_{4,Sq}$ islands follows a chain, with second- and third-order coupling resulting from the products of this chain forming other island types as they decay.

The first and second stages are the domains where the physically observable recovery takes place. As the first stage is composed of several decay rates that are proportional to ν_1, the overall effect is exponential decay with a rate of the order of ν_1, but not any specific value. The second stage is where most cluster decay with a rate $2\nu_2$, and obviously the system has the same overall decay rate. Those clusters that have a different rate are so much lower in concentration that they cannot contribute any significant effect. In the 750-K case we present, the same can be said for the concentration of all cluster types once they become linked to the $Y_{4,Sq}$. However, as the qualitative behavior does not alter as the temperature is lowered the original argument suffices, although it is redundant at the current temperature.

There is a third stage of recovery, where the concentrations are much too low to be important, but it is interesting to note that it merely reinforces the link of the now-universal $2\nu_2$ decay rate. In this third stage, the adatom concentration reaches its constant equilibrium concentration, which is determined by attachment and detachment processes of the adatoms at the step edges. Since the adatom concentration is now constant, this removes the second- and third-order coupling in the decay and formation chain shown in Fig. 8, and the decay of all the side products of the breakup of $Y_{4,Sq}$ follows the rate $\exp(-2\nu_2 t)$. From this stage each cluster type continues to decay at the same rate until it reaches its equilibrium concentration.

The above results show that it is crucial to include configurations with slow-decay pathways in models of the surface recovery. Since the decay of all of the other clusters couple to the slow decay of the stable species, the surface takes much longer to relax than would be predicted if only the fast-decay pathways were included, as was done in previous work. This leads to longer expected times for the settling of the surface morphology to its equilibrium stage, and greater surface coverage during the relaxation period.

IV. CONCLUSIONS

It is evident from the discussion in Sec. III that certain configurations with slow-decay pathways are very important for describing relaxation processes. Consequently, one might question our restriction of the island size to only four atoms, since a rectangular six-atom island has a slow-decay rate similar to that of a square four-atom island (there is no possible stable shape for a five-atom cluster, since at least one constituent atom will have only one nearest-neighbor bond to the cluster). However, regardless of the size of the cluster its fastest decay rate can never be slower than ν_2 and will link to smaller clusters in much the same way as $Y_{4,\mathrm{Sq}}$; thus, the general behavior will not be altered. In addition, the relative concentrations of different size clusters is a strong function of the growth conditions.[9,10] Near the step propagation mode, the nucleation rate on the terraces is low, since most adatoms have sufficient mobility to incorporate into the step edges, and thus the coverage of large islands is so small that it is only necessary to consider clusters with a few atoms. The larger the cluster the smaller its coverage; at 750 K and $J=1$ monolayer/s, the total adatom coverage is several orders of magnitude bigger than the coverage of the four-atom clusters. Thus, under these conditions it is reasonable to neglect five-atom and higher-atom islands.[9] We emphasize that the above model with four-atom islands applies only to step-flow mode conditions; for modeling of recovery at lower temperatures, it would be necessary to include even larger islands.

To summarize our results, we have carried out a detailed study of the dynamics of cluster formation during MBE growth and recovery on stepped surfaces. The consideration of the various cluster configurations for up to four-atom clusters provides a realistic model of growth on stepped surfaces under certain conditions, namely, near the step propagation mode where the total amount of nucleation on the terraces is small. We have elucidated the role of different island types and shapes during the various stages of growth. In the early stages, the less stable species with the highest formation rates are most important. During the recovery, stable configurations with slow-decay pathways dominate the relaxation of the surface. We have shown that the recovery of the surface can be divided into stages. The first stage is the fast cluster decay caused by the activity of atoms with one nearest-neighbor bond, and the next stage is dominated by the slower breakup of atoms with two nearest-neighbor bonds with a cluster. Decay of all of the clusters on the terraces in the second stage is coupled up to third order to the breakup of the most stable species. This finding supports earlier Monte Carlo simulations of recovery kinetics,[12,19] where it was also found that recovery proceeds by an initially rapid response, followed by a much slower process.

ACKNOWLEDGMENTS

S. K. Would like to thank the Nuffield Foundation for support administered through the Imperial College Undergraduate Research Opportunities Programme. This research was also supported in part by Imperial College and the Research Development Corporation of Japan under the auspices of the "Atomic Arrangement: Design and Control for New Materials" Joint Research Program.

[1] J. H. Neave, P. J. Dobson, B. A. Joyce, and J. Zhang, Appl. Phys. Lett. **47**, 100 (1983).
[2] A. K. Myers-Beaghton and D. D. Vvedensky, Phys. Rev. B **42**, 5544 (1990).
[3] W. K. Burton, N. Cabrera, and F. C. Frank, Philos. Trans. R. Soc. London. Ser. A **243**, 299 (1951).
[4] K. Voightlaender and H. Risken, Appl. Phys. A **39**, 31 (1986).
[5] V. Fuenzalida and I. Eisele, J. Cryst. Growth **74**, 597 (1986).
[6] V. Fuenzalida and I. Eisele, in *Proceedings of the First International Symposium on Silicon Molecular Beam Epitaxy*, edited by J. C. Beam, S. S. Iyer, E. Kasper, and Y. Shiraki (Electrochemical Society, Pennington, NJ, 1985), pp. 86–92.
[7] R. Ghez and S. S. Iyer, IBM J. Res. Dev. **32**, 804 (1988).
[8] S. Stoyanov, Appl. Phys. A **50**, 349 (1990).
[9] A. K. Myers-Beaghton and D. D. Vvedensky, Phys. Rev. A **44**, 2457 (1991).
[10] V. Fuenzalida, Phys. Rev. B **44**, 10 835 (1991).
[11] S. Clarke, D. D. Vvedensky, and M. W. Ricketts, J. Cryst. Growth **95**, 28 (1989).
[12] S. Clarke, D. D. Vvedensky, and Appl. Phys. Lett. **51**, 340 (1987).
[13] M. Ichikawa and T. Doi, Appl. Phys. Lett. **50**, 1141 (1987).
[14] C. W. Gardiner, *Handbook of Stochastic Methods* (Springer, Berlin, 1983).
[15] J. A. Venables, G. D. T. Spiller, and M. Hanbücken, Rep. Prog. Phys. **47**, 399 (1984).
[16] A. Zangwill, C. N. Luse, D. D. Vvedensky, and M. R. Wilby, in *Interface Dynamics and Growth*, edited by K. S. Liang, M. P. Anderson, R. F. Bruinsma, and G. Scoles, MRS Symposia Proceedings (Materials Research Society, Pittsburgh, 1992), pp. 189–198.
[17] J. H. Neave, B. A. Joyce, P. J. Dobson, and N. Norton, Appl. Phys. A **31**, 1 (1983).
[18] B. F. Lewis, F. J. Grunthaner, A. Madhukar, T. C. Lee, and R. Fernandez, J. Vac. Sci. Technol. B **3**, 1317 (1985).
[19] D. D. Vvedensky and S. Clarke, Surf. Sci. **225**, 373 (1990).
[20] A. Yoshinaga, M. Fahy, S. Dosanjh, J. Zhang, J. H. Neave, and B. A. Joyce, Surf. Sci. **264**, L157 (1992).

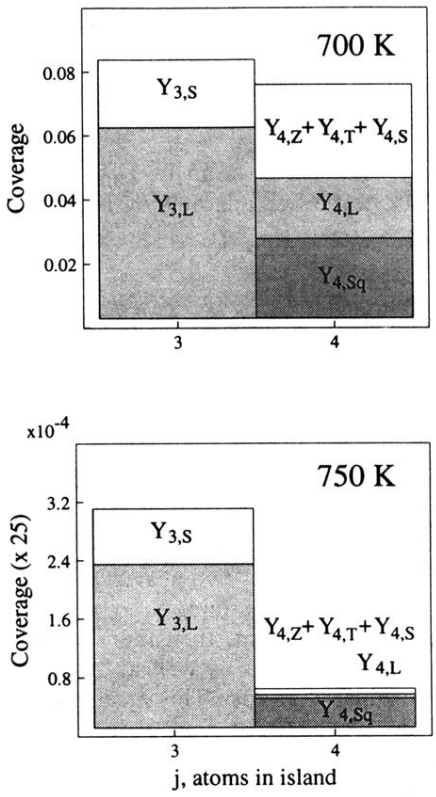

FIG. 6. Steady-state coverages for three- and four-atom clusters at $T=700$ and 750 K with the same parameters and growth conditions as for Fig. 5. Note the difference in scale; the results at 750 K are magnified 25 times with respect to those at 700 K.